Processing and Application of Ceramics 14 [3] (2020) 260–267
https://doi.org/10.2298/PAC2003260S

Structure and dielectric properties of Sm^{3+} modified $Bi_4Ti_3O_{12}$-$SrBi_4Ti_4O_{15}$ intergrowth ferroelectrics

Badavath Shobhan Babu, Simhachalam Narendra Babu, Guduru Prasad, Gobburu S. Kumar, Nandiraju V. Prasad*

Material Research Laboratory, Department of Physics, Osmania University, Hyderabad 500007, India

Received 1 April 2020; Received in revised form 17 June2020; Accepted 27 July 2020

Abstract

Novel samarium modified intergrowth ferroelectric ceramics, namely $Bi_4Ti_3O_{12}$-$SrBi_4Ti_4O_{15}$, were synthesized by conventional solid state reaction method and sintered at 1100 °C for 5 h. X-ray diffraction studies revealed the formation of a single phase with the signature of intergrowth oxide and plate like morphology was observed by scanning electron microscopic analyses. The orthorhombicity, the grain size and transition temperature were found to decrease with the increase of Sm content. The dielectric and modulus measurements were performed at different temperatures and frequency ranges. The transition temperature was found to be around 500 °C. The variations of imaginary part of modulus and dielectric constant with the temperature showed diffuse phase transition. The results are corroborated to the defect based mechanism and Curie deviation factor was evaluated by using the modified Curie-Weiss law. Polarization-electric filed curves displayed a typical narrow hysteresis loop at room temperature by applying an electric field of 70 kV/cm. However, above room temperature the hysteresis loop area was found to be increased. The overall results revealed that the complex dipoles and oxygen vacancies are playing a dominant role in the dielectric and electrical properties, and therefore the adopted intergrowth processing was found to be an effective approach to obtain potentially good ferroelectric materials.

Keywords: *BLSF, intergrowth ferroelectrics, dielectric and ferroelectric properties, relaxor-like behaviour*

I. Introduction

Bismuth layered-structure ferroelectric materials (BLSF), belonging to the Aurivillius family with intergrowth structure, are very attractive for high temperature piezoelectric and ferroelectric random access memory devices (FRAM) [1,2]. The structure of the compound consists of pseudo pervoskite layers $(A_{n-1}B_nO_{3n+1})^{2-}$ sandwiched between $(Bi_2O_2)^{2+}$ layers along *c*-axis [3]. It should be noted that A-site cation has 12-fold coordination and B-site cation is in 6-fold coordination. The term "n" represents the number of layers present in the formula. Rare earth modified $Bi_4Ti_3O_{12}$ ceramics are well-known materials for memory devices [4–6]. Thus, $SrBi_4Ti_4O_{15}$ compound, having four layered structure (n = 4), showed polarization along *c*-axis owing to the fact that it has orthorhombic crystalline structure [7]. Rare earth doped BLSF compounds have large remnant polarization (P_r) compared to other BLSF layered materials [8]. It has been reported that $SrBi_4Ti_4O_{15}$ compound has high insulating properties, compared to $Bi_4Ti_3O_{12}$. Therefore, continuous efforts are made to investigate the intergrowth compounds of these mixed layers [8–12]. In order to enhance the ferroelectric properties, generally two methods are adopted: i) thin-film route and ii) intergrowth route [2]. Recently, considerable attention has been paid to intergrowth ferroelectric ceramics in order to enlarge the ferroelectric and fatigue-free properties [2, 11–14]. In addition, many researchers have reported that one-half unit cell of *n*-layered structure combined with another (n+1)-layered structure along *c*-axis is an effective approach to enhance potential for ferroelectric applications [12–14].

Based on the theoretical equilibrium energies of various phases of higher layered-pervoskites of the Aurivillius and Ruddlesden-Popper materials, it is believed that the resulting mixed materials are observed to be

* Corresponding authors: tel: +91 9849553669,
e-mail: *nvp1969@rediffmail.com*

intergrowth compounds [15,16]. Moreover, the synthesis part is considered to be complex and challenging for compounds with higher number of layers ($n > 4$). Zhu *et al*. [8] reported that La-modified intergrowth compound, such as $SrBi_{8-x}La_xTi_7O_{27}$ with $x = 0.5$, has shown higher $2P_r$ (25.6 μC/cm^2) value. In their investigation, they found that rare earth (La) played a role in increasing $2P_r$ value by 60%, compared to the parent compounds.

Due to its potential for ferroelectric application, in the present investigation we have prepared intergrowth ferroelectrics based on Sm-doped mixed layered $Bi_4Ti_3O_{12}$-$SrBi_4Ti_4O_{15}$. One can speculate that the substitution of Bi^{3+} (1.17 Å) with smaller size Sm^{3+} (1.27 Å) can effectively stabilize the oxygen ion in the lattice and lead to improved dielectric and ferroelectric properties. Since A-site substitution is expected to significantly affect macroscopic properties, in this study, A-site modified three-layered ($Sm_xBi_{4-x}Ti_3O_{12}$ where $x = 0$, 0.37, 0.57 and 0.72; SBT) and four-layered ($SrSm_yBi_{4-y}Ti_4O_{15}$ where $y = 0$, 0.13, 0.43 and 0.78; SBST) compounds were prepared. The intergrowth SBT-SBST was fabricated by mixing the above mentioned two compounds. Detailed dielectric and ferroelectric properties were investigated.

II. Materials and methods

SBT ($Sm_xBi_{4-x}Ti_3O_{12}$, $x = 0$, 0.37. 0.57 and 0.72) and SBST ($SrBi_{4-y}Sm_yTi_4O_{15}$, $y = 0$, 0.13, 0.43, 0.78) precursor mixtures were prepared by the traditional solid state reaction. The starting oxides of AR grade with 99.99% purity of Bi_2O_3, Sm_2O_3, TiO_2 and $SrCO_3$ were taken in stoichiometric ratios and mixed thoroughly, using agate mortar and pestle. Intergrowth $Sm_xBi_{4-x}Ti_3O_{12}$-$SrBi_{4-y}Sm_yTi_4O_{15}$ samples (SBT-SBST, where total Sm contents $x + y$ are 0, 0.5, 1.0 and 1.5) were obtained by mixing the SBT and SBST phases (Table 1). The reactants were mixed thoroughly using agate mortar and pestle. The dried mixtures were calcined at 900 °C for 5 h. Requisite amount of polyvinyl alcohol (2 wt.%) was added as a binder before making the final pellets. Circular shaped pellets were obtained by applying approximately uniaxial pressure of 300 MPa. The pellets were finally sintered at 1100 °C for 5 h.

Phase analysis was performed by XRD studies made at room temperature on the calcined and sintered powder samples. Electrical measurements were obtained by using impedance analyser HP4192A and Marine India Loop Tracer. Before measurements, the pellets were coated with silver paste. Detailed dielectric, impedance and ferroelectric properties of the intergrowth ferroelectrics (SBT-SBST) were studied.

III. Results and discussion

3.1. Structural characterization

Figure 1a shows XRD patterns (measured at room temperature) of the SBT samples with different Sm contents. All diffraction peaks were indexed with the parent $Bi_4Ti_3O_{12}$ compound and there is no considerable change in the structure of $Bi_4Ti_3O_{12}$ after Sm-substitution at the Bi-site. This is clearly confirmation that the samarium ion readily replaces bismuth ion in the structure. However, the intensities of diffraction peaks corresponding to (00*l*) plane decrease with increasing Sm addition, which may be due to the reduction of grain growth along the preferred (00*l*) planes. The results are consistent with our earlier report [17].

XRD patterns of the SBST samples with different Sm contents are shown in Fig. 1b. The Aurivillius crystalline structure of SBST was indexed based on the parent $SrBi_4Ti_4O_{15}$ compound, whose space group is $A2_iam$ [18]. The intensity of the diffraction peaks corresponding to (006), (008), (0010) and (0022) planes increase with increasing the incorporation of Sm in the SBST lattice. The lattice parameters of the $SrBi_{3.22}Sm_{0.78}Ti_4O_{15}$ compound were found to be a = 5.4520, b = 5.4377 and c = 41.5883 Å. The lattice parameter a is larger when compared to the parameter b and there was no much variation seen in the other lattice parameters of SBST. The maximum peak intensities observed for the SBT and SBST samples, corresponding to (117) and (119) planes, are consistent with the strong diffraction peaks of the parent compounds ($Bi_4Ti_3O_{12}$ and $SrBi_4Ti_4O_{15}$).

XRD pattern of the calcined intergrowth SBT-SBST samples at 900 °C (Fig. 1c) clearly confirms the formation of a single phase structure and the detected peaks were indexed according to the standard powder diffraction pattern of $SrBi_8Ti_7O_{27}$. The lattice parameters were also calculated based on the parent compound and determined data are given in Table 2. The strongest diffraction peaks of SBT ($n = 3$) and SBST ($n = 4$) are known to occur at (11 2n+1) and therefore the strongest XRD peak of intergrowth compound is located between 117 and 119 or $hk\,l+1$ reflections. In addition, the full width at half maximum value of the strongest XRD peak was found to increase with the increase of Sm content (i.e.

Table 1. Sample notation

Sample composition	Total Sm content $x + y$	Sample notation
$Bi_4Ti_3O_{12}$-$SrBi_4Ti_4O_{15}$	0.0	0-SBT-SBST
$Sm_{0.37}Bi_{3.63}Ti_3O_{12}$-$SrSm_{0.13}Bi_{3.87}Ti_4O_{15}$	0.5	0.5-SBT-SBST
$Sm_{0.57}Bi_{3.43}Ti_3O_{12}$-$SrSm_{0.43}Bi_{3.57}Ti_4O_{15}$	1.0	1-SBT-SBST
$Sm_{0.72}Bi_{3.28}Ti_3O_{12}$-$SrSm_{0.78}Bi_{3.22}Ti_4O_{15}$	1.5	1.5-SBT-SBST

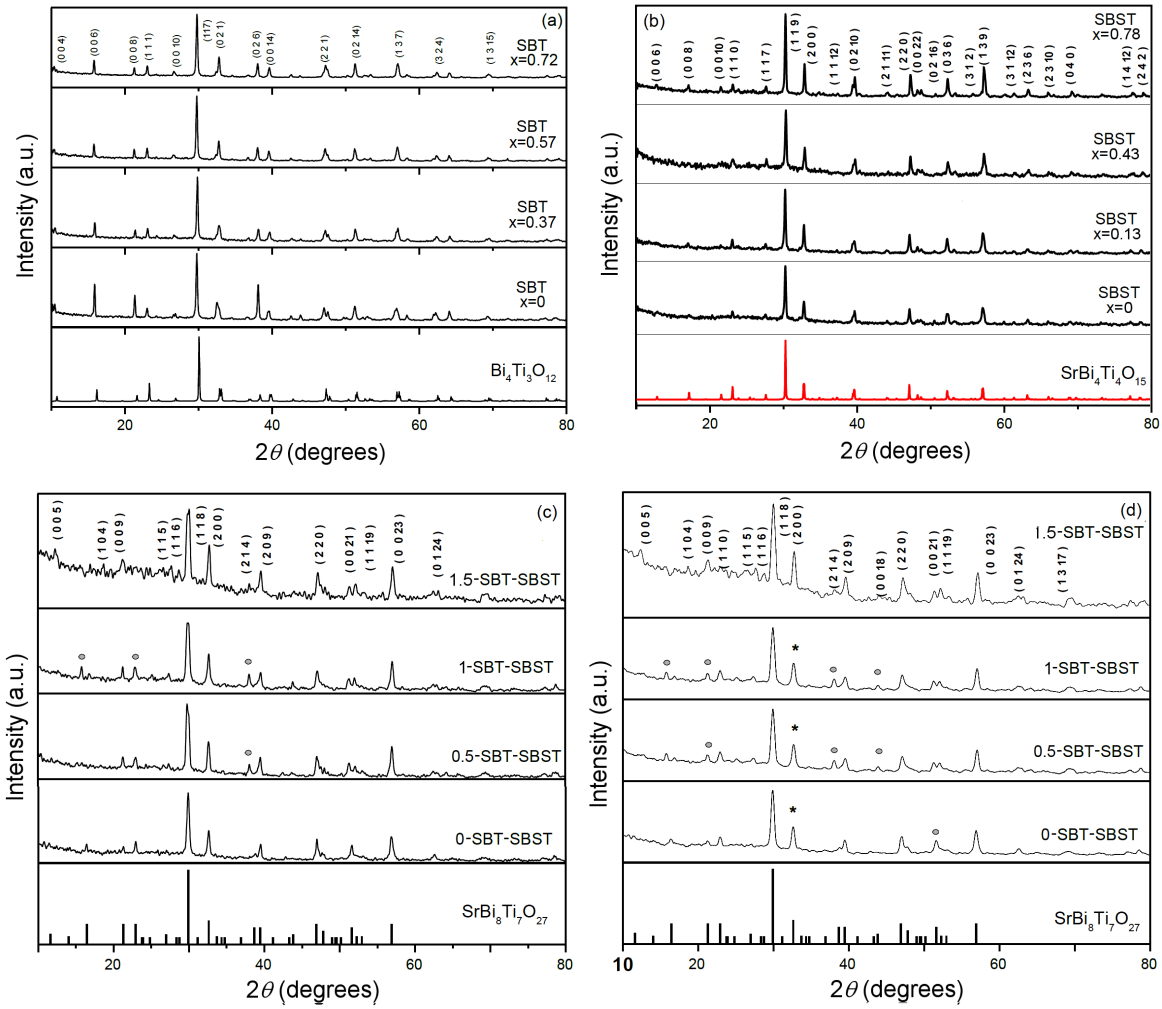

Figure 1. XRD patterns of a) SBT, b) SBST, c) calcined SBT-SBST and d) sintered SBT-SBST samples

Table 2. Lattice parameters and orthorombicity (*Or*) of intergrowth SBT-SBST ceramics *vs*. Sm content ($x + y$)

Sample composition	Total Sm content	Lattice parameter [Å]			*Or*
	$x + y$	*a*	*b*	2*c*	
0-SBT-SBST	0.0	5.4530	5.4415	76.978	0.00211
0.5-SBT-SBST	0.5	5.4515	5.4415	74.074	0.00184
1-SBT-SBST	1.0	5.4515	5.4415	74.946	0.00184
1.5-SBT-SBST	1.5	5.4515	5.4386	74.074	0.00237
SrBi4Ti7O27	0.0	5.4500	5.4400	73.990	0.00184

$x + y$ value). This is thought to be due to the formation of intergrowth structure.

The XRD patterns of the SBT-SBST samples sintered at 1100 °C (Fig. 1d) consist all major phases and secondary phases: $Bi_2Ti_2O_7$ (marked as open circles) and SBST (marked as stars). It was reported that Sm^{3+} can replace easily all Bi^{3+} ions at the A-site as well as Bi^{3+} sites of $(Bi_2O_2)^{2+}$ in $Bi_4Ti_3O_{12}$ [4,5]. However, the same is not the case for SBT-SBST or $SrBi_8Ti_7O_{27}$ (higher layer-structured, $n > 4$, materials). Therefore, it should be remembered here that a mixed (intergrowth) layered structure may not be stable as ordinary bismuth layer structure. The basic reason is attributed to the size mismatch of one-half unit cell of SBT and another one-half unit cell of SBST. In order to extract more information, the orthorhombicity of the present layered pervoskite was evaluated by using the following formula:

$$Or = \frac{2(a-b)}{a+b} \tag{1}$$

The lattice parameters and orthorhombicity of $SrBi_8Ti_7O_{27}$ are also given in Table 2, for comparison with the SBT-SBST. From Table 2, it is observed that the relaxation of structural distortion (orthorhombicity) is more or less the same for all the compositions except for the samples with Sm content of 0 and 1.5. This is attributed to the shrinkage of *c*-lattice parameter. Since the bond distance of Sm–O is shorter than Ti–O

hybridization, the substitution of smaller ion Sm^{3+} for Bi^{3+} might cause changes in structural-distortion and ferroelectric properties [19–22]. The peak magnitude of (200) plane reflection (shown in Fig. 1d) is found to be increased. This clearly states that the grain growth mechanism is restricted along *a*- and *b*-directions, which is being considered as characteristic feature of these compounds. The splitting of the peak near 2θ of 50° is clearly observed with increasing the Sm^{3+} content in the compounds. Since the radius of Sm^{3+} ion (1.24 Å) is smaller than the Bi^{3+} ion (1.35 Å), it should be noted here that Sm^{3+} ion may be unavoidably incorporated into $(Bi_2O_2)^{2+}$ layers with increasing Sm^{3+} concentration in the SBT- SBST intergrowth formula. This kind of phenomenon is attributed to the different chemical nature of Bi^{3+} and Sm^{3+} ions. Another possible reason could be the effect of $6s^2$ lone pair electron for Bi^{3+} ion and the lattice mismatch of SBT-SBST, which is sandwiched between $(Bi_2O_2)^{2+}$ layers. In addition, Bi^{3+} has lone-pair electrons whereas Sm^{3+} ion may not have any lone pair electrons. If the substitution of Sm^{3+} breaks the crystalline structure of $(Bi_2O_2)^{2+}$ layers, then one should get a shift towards the maximum peak position at higher 2θ angle. Therefore, a slightly broader peak observed near 30° of 2θ is a clear indication of signature behaviour of mixed kind intergrowth polycrystalline nature.

Figure 2 shows SEM pictures of the SBT-SBST fractured surfaces. It is a well known that the sintering mechanism is mainly concerned with the reaction between the reactants. Moreover, these materials used to have anisotropic crystal structure with lower surface energy of (00*l*) planes, which leads to an easy grain growth in *ab*-plane and finally develops plate like morphology. The SEM photographs show typical plate-like structure and the average grain size is found to decrease from 3 to 1 μm, with increasing Sm concentration in the SBT-SBST intergrowth composition. This clearly indicates that Sm^{3+} acts as an inhibiter of the grain growth. The decrease of the preferred orientation of (0018) plane (Fig. 1d) indicates the reduction of the preferential growth of plate-like morphology, as seen in the SEM images. However, the tendency of the grain orientation towards long *c*-axis, normal to the *ab*-plane, and decreasing the *c*-parameter with increasing the Sm concentration (i.e. $x + y$ value) is observed. The results are evident with decreasing the thickness of the grain and a slight variation of density form 94 to 96%, calculated from the experimental and theoretical values.

3.2. Dielectric and ferroelectric properties

As mentioned earlier, the dielectric properties of SBT-SBST ceramics are related with two factors: i) tilting of TiO_6 octahedron and ii) lattice mismatch between the two different layered compounds (SBT and SBST). Figure 3 shows the temperature dependent permittivity (ε') and dielectrics loss for the intergrowth SBT-SBST compositions measured at 10, 50 and 100 kHz. The

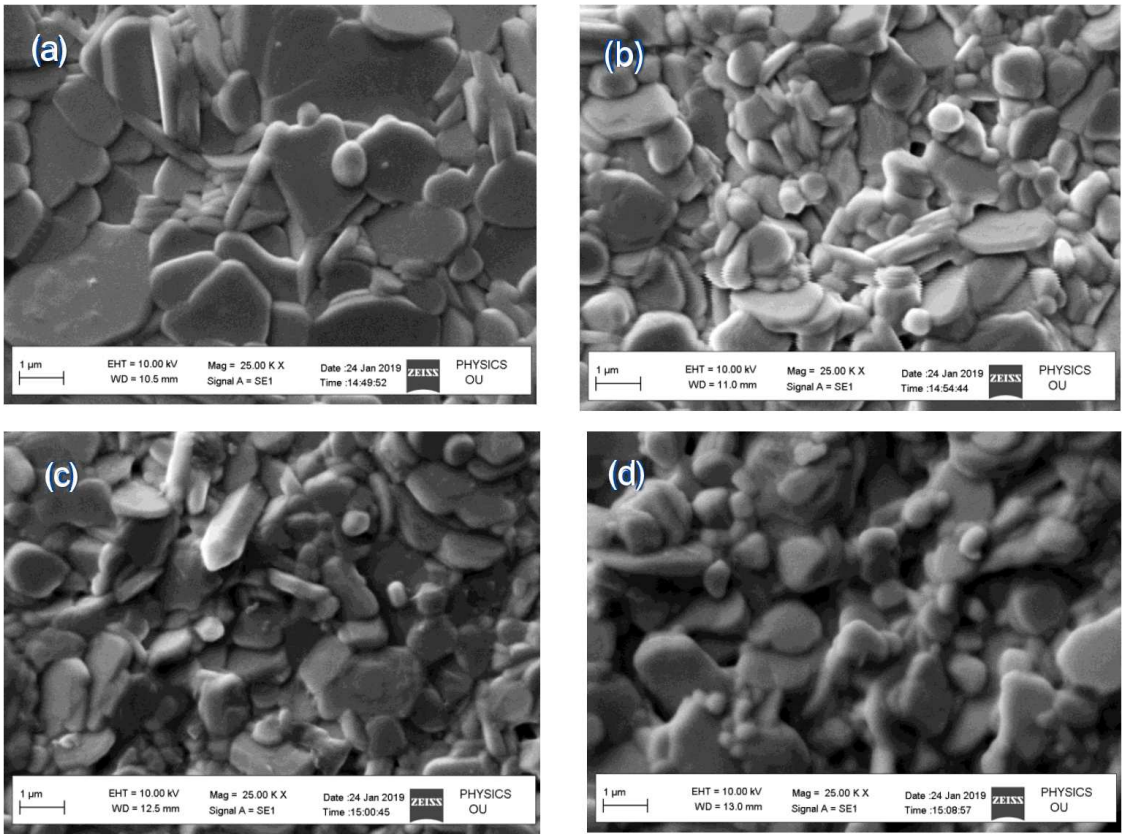

Figure 2. SEM micrographs of SBT-SBST sintered samples: a) 0-SBT-SBST, b) 0.5-SBT-SBST, c) 1-SBT-SBST and d) 1.5-SBT-SBST

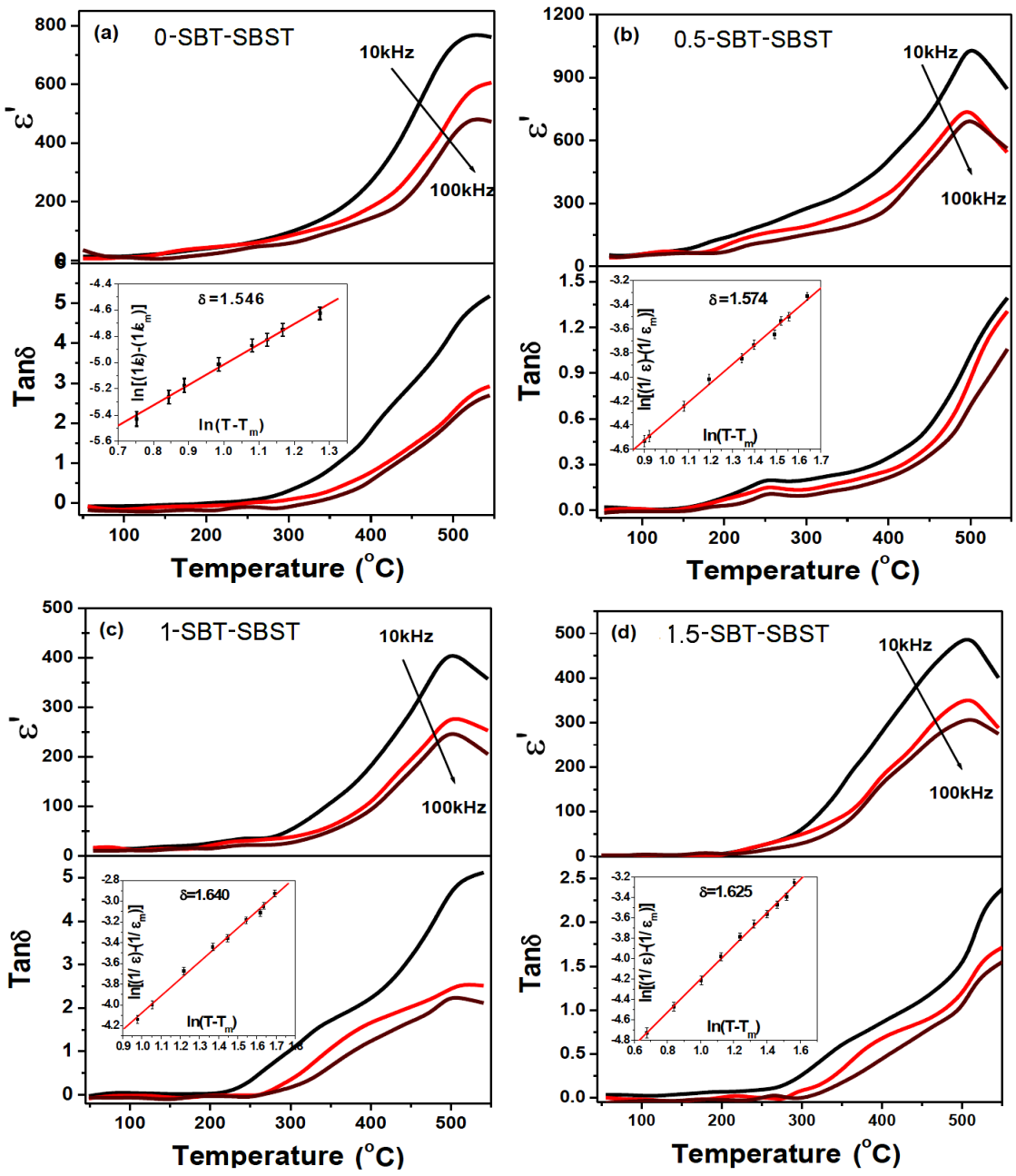

Figure 3. Dielectric constant and dielectric loss versus temperature for sintered SBT-SBST samples: a) 0-SBT-SBST, b) 0.5-SBT-SBST, c) 1-SBT-SBST, and d) 1.5-SBT-SBST (insets present $\log(1/\varepsilon' - 1/\varepsilon'_{max})$ *vs.* $\log(T - T_{max})$)

Table 3. Transition temperature (T_C), deviation factor (γ) and tolerance factor (t) values of SBT-SBST intergrowth ceramics

Intergrowth composition $SrSm_xBi_{8-x}Ti_7O_{27}$	T_C [°C]	t	γ (at 100 kHz)
0-SBT-SBST	522	0.925	1.54
0.5-SBT-SBST	500	0.934	1.57
1-SBT-SBST	497	0.944	1.64
1.5-SBT-SBST	508	0.953	1.62

observed increase in dielectric loss with the temperature increase is attributed to the increase of conductivity. The dielectric constant decreases with increasing frequency and Sm content. Dielectric curves are characterized with diffuse nature which is attributed to the random distribution of two cations, namely Sr^{2+} and Sm^{3+}, at A (Bi^{3+})-site. The random distribution of cations also creates changes in ferroelectric phase transition temperature, as it is seen in Table 3. The diffuse phase transition nature can be evaluated by using the following modified Curie-Weiss law:

$$\frac{1}{\varepsilon'} - \frac{1}{\varepsilon'_{max}} = \frac{(T - T_{max})^{\gamma}}{C} \tag{2}$$

where ε' is dielectric constant, ε'_{max} is the maximum dielectric constant obtained at the transition temperature, C is the modified Curie-Weiss constant and γ is the deviation factor showing the degree of deviation from the

Curie-Weiss law. The variation of $\log(1/\varepsilon' - 1/\varepsilon'_{max})$ with $\log(T - T_{max})$ is shown for all the samples in insets of Fig. 3. The slope of the plot gives the value of γ which generally lies between 1 and 2. It is well-known fact that for normal ferroelectrics $\gamma = 1$ and in the case of ideal relaxors $\gamma = 2$. The values of deviation factor (γ) and transition temperature are depicted in Table 3. The value of γ is found to increase with increasing Sm content, which may be due to the rapid changes in the tolerance factor of the pervoskite units (Table 3). It should be noted here that the tolerance factor for most of the distorted pervoskites should be around 0.9 ($0.8 < t < 1$). The tolerance factor of the investigated SBT-SBST compounds was calculated by using the following modified formula:

$$t = \frac{R_O + R_{Sr^{2+}} + (2-x)R_{Bi^{3+}} + xR_{Sm^{3+}}}{\sqrt{2(R_O + (4-\gamma)R_{Ti^{4+}})}} \qquad (3)$$

where R_O is oxygen ion radius, $R_{Sr^{2+}}$, $R_{Bi^{3+}}$, $R_{Sm^{3+}}$ are the effective A-site ionic radii and $R_{Ti^{4+}}$ is B-site (Ti-ionic) radius. The tolerance factor for all the compositions is shown in Table 3. More diffused nature and smaller grain size of the 1.5-SBT-SBST sample could be attributed to decreased amount of oxygen vacancies.

In order to extract more information about electric behaviour of the processed SBT-SBST ceramics, modulus plots (complimentary to the dielectric) are shown in Fig. 4. The modulus (M^*), impedance (Z^*) and dielectric (ε^*) relation is shown in the following equation:

$$M^* = \frac{1}{\varepsilon^*} = j \cdot \omega \cdot C_0 \cdot Z^* \qquad (4)$$

where C_0 represents the geometrical capacitance and $\omega = 2\pi f$.

Variation of the real part of modulus with temperature is shown in Fig. 4. A noteworthy aspect from the plot is that the M' is found to decrease with increasing temperature and attaines almost a constant value at higher temperature. This characteristic kind of behaviour is attributed to the diffused phase transition nature of the sample.

Figure 5 shows the hysteresis (P vs. E) loop for all

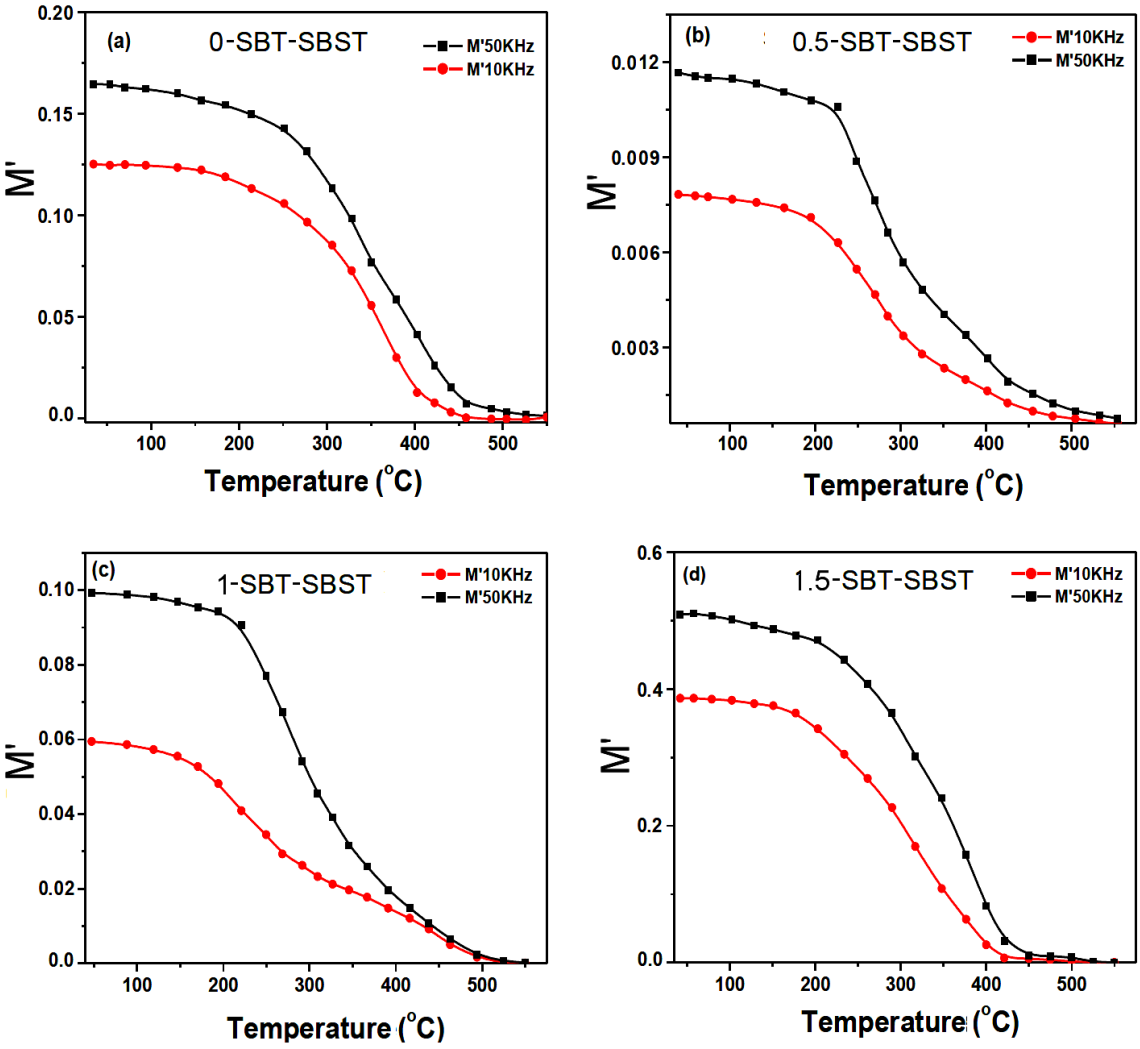

Figure 4. The variation of the real part of modulus (M') with temperature for sintered SBT-SBST intergrowth samples: a) 0-SBT-SBST, b) 0.5-SBT-SBST, c) 1-SBT-SBST and d) 1.5-SBT-SBST

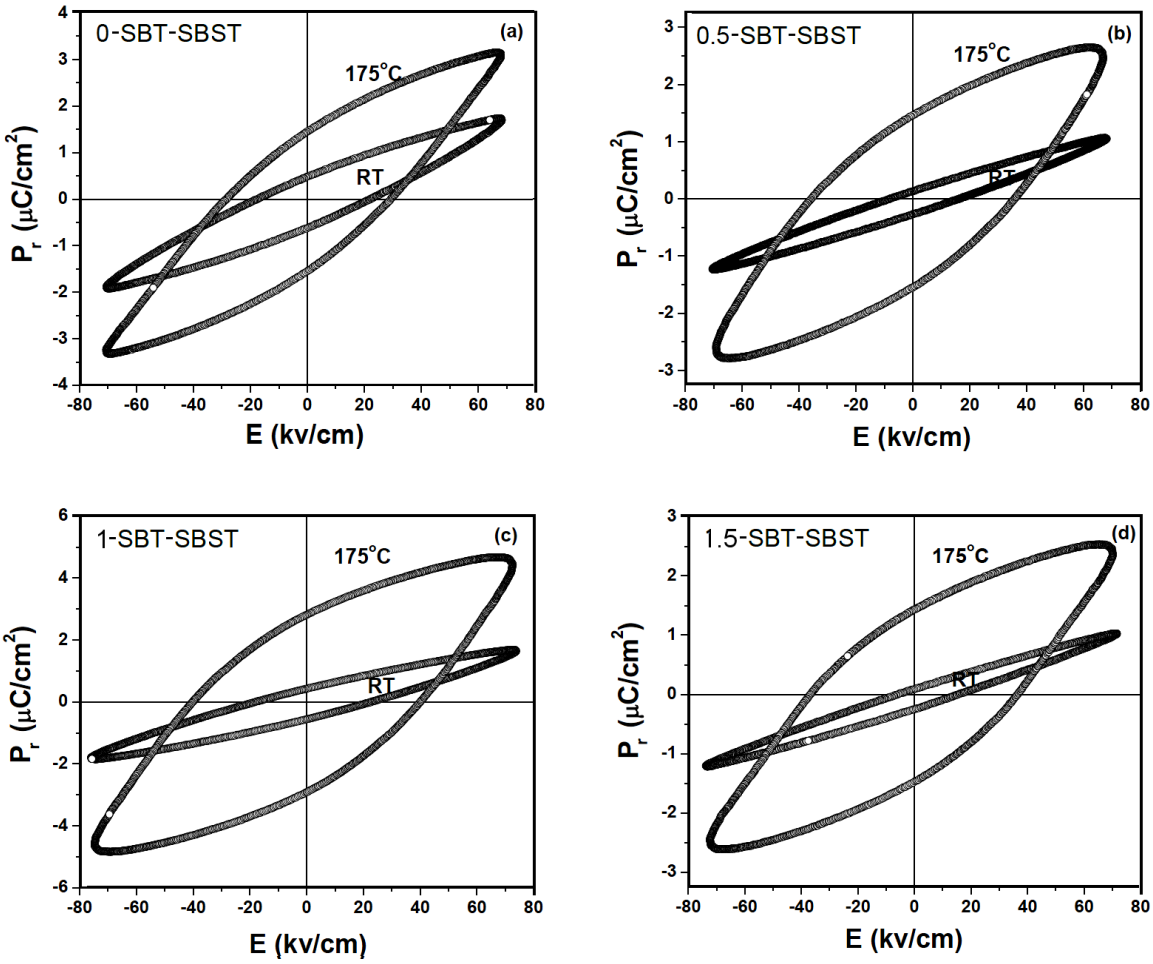

Figure 5. Hysteresis loops for sintered SBT-SBST samples: a) 0-SBT-SBST, b) 0.5-SBT-SBST, c) 1-SBT-SBST and d) 1.5-SBT-SBST

the intergrowth samples, under the applied electric field up to 70 kV/cm. These loops are not saturated due to the low applied field, which was the limitation of the conducted experiments. However with the increase of temperature, the loop area is found to be larger. The increase of the P_r value with temperature is attributed to the increase diffusive nature as well as the ferroelectric nature of the samples. The results are consistent with the dielectric and modulus plots (Figs. 3 and 4). Substitution of Sm might acts as the resistant to the oxygen vacancies and intern decreases the space charge effects.

Based on this, one can speculate that higher Sm^{3+} content in the unit cell (i.e. in the sample 1.5-SBT-SBST) showed more diffusive behaviour, which was seen in the dielectric, modulus and ferroelectric hysteresis results. The diffusive nature might be also attributed to the volatile nature of Bi during the sintering process. According to the following Kroger-Vink reaction (Eq. 5), one can speculate that the number of oxygen vacancies becomes higher at higher temperatures.

$$2\,Bi_{Bi}^{x} + 3\,O_{O}^{x} \longrightarrow 2\,V_{Bi}''' + 3\,V_{O}'' + Bi_2O_3\uparrow \qquad (5)$$

Based on the above Kroger-Vink notation, one can speculate that the double positive oxygen vacancy (V_O'') can easily compensate with titanium ion and maintain the charge neutrality condition [22]. The complex defect dipoles such as Ti^{3+}–V_O'' and Ti^{4+}–V_O'', play an important role in the conduction process at lower temperature. As temperature increases the double ionized vacancies become single ionized vacancy and electron. They start playing a role in the conduction process at higher temperatures. From this, one can speculate that the substitution of Bi^{3+} with Sm^{3+} ion could improve ferroelectric properties, which can be attributed to the reduction of oxygen vacancy concentration. This in turn leads to the weakening of the defect mobility and domain pinning effect and results in the well-defined hysteresis behaviour at higher temperatures. The results can be attributed to the increasing stabilization of the 1.5-SBT-SBST, due to the substitution of Bi^{3+} with chemically stable Sm^{3+} ion. The results can be corroborated with the tolerance factor values and rotation of octahedral (TiO_6).

IV. Conclusions

SBT-SBST intergrowth ceramics belonging to bismuth layered-structure ferroelectric materials were prepared. X-ray diffraction confirms the formation of single

phase intergrowth ceramics. Orthorhombic distortion is found to decrease with increasing the Sm^{3+} concentrations. The related strong XRD peaks corresponding to (118), (200), and (209) planes are found to increase with increasing Sm content. An increase in full width at half maximum value of the strongest XRD peak is attributed to the characteristic nature of intergrowth. SEM micrographs show typical plate-like structure and the grain size is found to decrease with increasing Sm concentration in the SBT- SBST intergrowth. The temperature variation of dielectric constant and M' vs. temperature plots shows a diffusive phase transition. An increase in dielectric loss with increasing the temperature is attributed to the increasing of the conductivity of the sample. From the modulus plot, complimentary to dielectric permittivity data, the transition temperature is found to be approximately in the range of 490–520 °C. The remnant polarization P_r is found to increase with increasing the temperature. The diffusivity parameter, obtained from the dielectric data at 100 kHz, is also found to increase with increasing the Sm concentration. Based on this one can speculate that the adopted intergrowth might be promising and effective approach in preparing potentially good intergrowth ferroelectric materials.

Acknowledgements: The research work is partially financed by the grants from the OU-DST PURSUE programme, India (No. C-DST-PURSE-II/07/2018).

References

1. U. Chon, K. Bum Kim, H. . Jang, G. Yi, "Fatigue-free samarium-modified bismuth titanate ($Bi_{4-x}Sm_xTi_3O_{12}$) film capacitors having large spontaneous polarizations", *Appl. Phys. Lett.*, **79** [19] (2001) 3137–3139.
2. H. Yang, Z. Chen, R. Peng, H. Haung, Z. Fu, X. Zhai, Y. Lu, "Super lattice-like structure and enhanced ferroelectric properties of intergrowth Aurivillius oxides", *RSC Adv.*, **8** (2018) 16937–16946.
3. B. Aurivillius, "Mixed bismuth oxides with layer lattices I. The structure type of $CaNb_2Bi_2O_9$", *Arkiv Kemi*, **1** (1949) 463–480.
4. B.H. Park, B.S. Kang, S.D. Bu, T.W. Noh, J. Lee, W. Jo. "Lanthanum-substituted bismuth titanate for use in non-volatile memories", *Nature*, **401** (1999) 682–684.
5. H.N. Lee, D. Hesse, N. Zakharov, U. Gosele, "Ferroelectric $Bi_{3.25}La_{0.75}Ti_3O_{12}$ films of uniform *a*-axis orientation on silicon substrates", *Science*, **296** [5575] (2002) 2006–2009.
6. H. Hao, H.X. Liu, M.H. Cao, S.X. Ouyang, "Lead-free $SrBi_4Ti_4O_{15}$ and $Bi_4Ti_3O_{12}$ material fabrication using the microwave-assisted molten salt synthesis method", *J. Am. Ceram. Soc.*, **90** [5] (2007) 1659–1662.
7. X.-B. Chen, R. Hui, J. Zhu, W.-P. Lu, X.-Y. Mao, "Relaxor properties of lanthanum-doped bismuth layer-structure ferroelectrics", *J. Appl. Phys.*, **96** [10] (2004) 5697–5700.
8. J. Zhu, X.-B. Chen, R. Hui, "Properties of lanthanum-doped intergrowth ferroelectrics", *Appl. Phys. Lett.*, **83** (2003) 1818–1820.
9. T. Wei, C.Z. Zhao, C.P. Li, Y.B. Lin, X. Yang, H.G. Tan, "Photoluminescence and ferroelectric properties in Eu doped $SrBi_4Ti_4O_{15}$-$Bi_4Ti_3O_{12}$ intergrowth ferroelectric ceramics", *J. Alloys Compd.*, **577** (2013) 728–733.
10. S.-P. Gu, W. Wang, J.-H. He, X.-B. Chen, "Ferroelectric, piezoelectric and dielectric properties of Nb modified $Bi_4Ti_3O_{12}$-$SrBi_4Ti_4O_{15}$ intergrowth", *Integr. Ferroelec.*, **94** (2007) 56–63.
11. Y. Jiang, X. Jiang, C. Chen, Y. Chen, X. Jiang, N. Tu, X. Xia, Y. Luo, S. Zhu, "Structural and electrical properties of La^{3+}-doped $Na_{0.5}Bi_{4.5}Ti_4O_{15}$-$Bi_4Ti_3O_{12}$ intergrowth high temperature piezo-ceramics", *Ceram. Int.*, **43** [8] (2017) 6446–6452.
12. Y. Noguchi, M. Miyayama, T. Kudo, "Ferroelectric properties of intergrowth $Bi_4Ti_3O_{12}$-$SrBi_4Ti_4O_{15}$ ceramics", *Appl. Phys. Letts.*, **77** (2000) 3639–3641.
13. G. Fan, X. Jiang, C. Chen, Y Chen, K. Du, N. Tu, X. Jiang, X. Xia, P. Wang, "Photoluminescence and electrical properties of Eu^{3+} doped $CaBi_8Ti_7O_{27}$ intergrowth ceramics", *J. Mater. Sci. Mater. Elect.*, **29** (2018) 6484–6490.
14. G.P. Choi, S.Y. Cho, S. Bu, "Structure and electrical properties of intergrowth bismuth layer-structured $Bi_4Ti_3O_{12}$-$CaBi_4Ti_4O_{15}$ ferroelectric ceramics", *J. Korean Phys. Soc.*, **69** (2016) 816–821.
15. R.J.D. Tilley, "An electron microscope study of pervoskite related oxides in Sr-Ti-O system", *J. Solid State Chem.*, **21** (1977) 293–301.
16. E.V. Ramana, N.V. Prasad, F. Figueiras, L. Lajaunie, R. Arenal, G. Otero-Irurueta, M.A. Valente, "The growth and improved magnetoelectric response of strain-modified Aurivillius $SrBi_{4.25}La_{0.75}Ti_4FeO_{18}$ thin films", *Dalton Trans.*, **48** (2019) 13224–13241.
17. B. Shoban Babu, G. Prasad, G.S. Kumar, N.V. Prasad, "Influence of samarium substitution on the ferroelectricity of $Bi_4Ti_3O_{12}$ ceramic", *Ferroelec.*, **517** (2017) 41–45.
18. E.C. Subba Rao, "A family of ferroelectric bismuth compounds", *J. Phys. Chem. Solids*, **23** (1962) 665–676.
19. R.Z. Hou, X.M. Chen, S.Y. Wu, "Substitution of Sm^{3+} and Nd^{3+} for Bi^{3+} in $SrBi_8Ti_7O_{27}$ mixed Aurivillius phase", *Jpn. J. Appl. Phys.*, **42** (2003) 5169–5171.
20. G. Parida, J. Bera, "Electrical properties of niobium doped intergrowth ferroelectrics", *Ceram. Int.*, **40** (2014) 3139–3144.
21. H. Hao, H. Liu, S. Ouyang, "Structure ferroelectric property of Nb-doped $SrBi_4Ti_4O_{15}$ ceramics", *J. Electroceram.*, **22** (2009) 357–362.
22. M. Afqir, A. Tachafine, D. Fasquelle, M. Elaatmani, J.C. Carru, A. Zegzouti, M. Daoud, S. Sayouri, "Structural, electric and dielectric properties of Eu-doped $SrBi_2Nb_2O_9$ ceramics obtained by co-precipitate route", *Process. Appl. Ceram.*, **12** (2018) 72–79.